Journal of Inflammation Research

Dovepress
open access to scientific and medical research

Open Access Full Text Article

ORIGINAL RESEARCH

Lycopus lucidus Turcz Exerts Neuroprotective Effects Against H_2O_2-Induced Neuroinflammation by Inhibiting NLRP3 Inflammasome Activation in Cortical Neurons

Hyunseong Kim[1]
Jin Young Hong[1]
Wan-Jin Jeon[1]
Junseon Lee[1]
Seung Ho Baek[2]
In-Hyuk Ha[1]

[1]Jaseng Spine and Joint Research Institute, Jaseng Medical Foundation, Seoul, 135-896, Republic of Korea; [2]College of Korean Medicine, Dongguk University, Goyang-si, 10326, Republic of Korea

Purpose: *Lycopus lucidus* Turcz (LLT) is a potent traditional medicinal herb that exerts therapeutic effects, regulating inflammatory disorders. However, the precise mechanisms by which LLT plays a potent role as an anti-inflammatory agent are still unknown, and in particular, the effects of LLT on cortical neurons and related mechanisms of neuroinflammation have not been studied. The NLRP3 inflammasome pathway is one of the most well known as an important driver of inflammation. We therefore hypothesized that LLT, as an effective anti-inflammatory agent, might have neurotherapeutic potential by inhibiting the NLRP3 inflammasome pathway in cortical neurons.

Materials and Methods: Primary cortical neurons were isolated from the embryonic rat cerebral cortex, and H_2O_2 was used to stimulate neuron damage in vitro. After treatment with LLT at three concentrations (10, 25, and 50 μg/mL), the expression of iNOS, NLRP3, ASC, caspase-1, IL-1β, IL-18, IL-6, and IL-10 was determined by immunocytochemistry, qPCR, and ELISA. Neuron apoptosis was also evaluated using Annexin V-FITC/PI double staining FACS analysis. Neural regeneration-related factors (BDNF, NGF, synaptophysin, NT3, AKT, and mTOR) were analyzed by immunocytochemistry and qPCR.

Results: LLT effectively protected cultured rat cortical neurons from H_2O_2-induced neuronal injury by significantly inhibiting NLRP3 inflammasome activation. In addition, it significantly reduced caspase-1 activation, which is induced by inflammasome formation and regulated the secretion of IL-1β/IL-18. We demonstrated that LLT enhances axonal elongation and synaptic connectivity upon H_2O_2-induced neuronal injury in rat primary cortical neurons.

Conclusion: It was first demonstrated in vitro that LLT suppresses NLRP3 inflammasome activation, attenuates inflammation and apoptosis, and consequently promotes neuroprotection and the stimulation of neuron repair, suggesting that it is a promising therapeutic for neurological diseases.

Keywords: *Lycopus lucidus* Turcz, cortical neuron, hydrogen peroxide, NLRP3 inflammasome, neuroinflammation

Introduction

Central nervous system (CNS) inflammation alters neurotransmission, affects neuronal death, regeneration, and neuroplasticity, and is involved in the pathophysiology of neurological diseases.[1,2] When activated by harmful stimuli, such as trauma, infection, and oxidative factors, inflammatory cells secrete abnormal levels of proinflammatory cytokines and amplify the response of other immune cells, leading

Correspondence: In-Hyuk Ha
Jaseng Spine and Joint Research Institute, Jaseng Medical Foundation, Seoul, 135-896, Republic of Korea
Tel +82-2-2222-2740
Fax +82-2-527-1869
Email hanihata@gmail.com

Received: 5 February 2021
Accepted: 7 April 2021
Published: 5 May 2021

to clinical symptoms of inflammation.[3,4] Recent studies have reported that neuroinflammation is related to inflammasome activation and IL-1β, IL-18, and IL-33 production.[5,6] Inflammasomes are complexes formed from homogeneous proteins expressed in inflammatory cells activated by specific stimuli. Activated inflammasomes induce the cleavage of procaspase-1 into active caspase-1, which cleaves IL-1β precursors generated by pattern recognition receptor-mediated signaling into IL-1β, the active form.[2,7,8] Thus, active cytokines produced by inflammasome activation are important drivers of inflammation that interact with other cytokine pathways to activate immune responses against infection and injury.[9] Inflammasomes have recently been implicated in the etiology, onset, and progression of several important diseases, in addition to being a novel biological defense mechanism against pathogens.[10] To date, multiple types of inflammasomes have been identified and studied, among which NLRP3 inflammasomes have been strongly associated with the progression and pathophysiological mechanisms of CNS disorders, such as Parkinson's disease, Alzheimer's disease, and stroke.[11–15] Previous studies have shown that inhibiting inflammasome activation after traumatic brain injury regulates neuroinflammatory responses by reducing neurodegeneration and cortical damage induced by injury.[16] Moreover, blocking the NLRP3 inflammasome and its adaptor protein ASC (the adaptor molecule apoptosis-associated speck-like protein containing a CARD) has been shown to induce against injury-induced neuroinflammatory responses by decreasing caspase-1, inducible nitric oxide synthase (iNOS), and IL-1β activation.[17,18] Therefore, it is important to understand these mechanisms to develop treatments for neurological diseases related to neuroinflammation. Based on these mechanisms, current studies are developing treatments for neuropathy based on natural substances with few side effects, for which safety and effectiveness have been empirically verified. Many herbal medicines are well known for their therapeutic properties related to the presence of phenolic compounds, especially phenolic acids and flavonoids.[19] Plant polyphenols have been reported to have key effects on cellular and body metabolism in response to oxidative stress and associated pathologies such as cancers, heart disease, and inflammation.[20] Syringic acid (4-hydroxy-3,5-di-methoxybenzoic acid) is one of the well-known polyphenolic natural compounds and is a therapeutic agent for various diseases.[21–23] Plants of the genus *Lycopus*, from the Lamiaceae family, are also natural sources rich in flavonoids, coumarins, terpenoids, and tannins, which can provide antioxidant and anti-inflammatory effects.[24] Therefore, *Lycopus lucidus* Turcz (LLT) has been widely used as a traditional and medicinal plant for centuries. It is well-known to have anti-oxidative and anti-inflammatory effects with respect to anti-inflammatory, wound, edema, menstrual disorder, abdominal pain, rheumatic arthritis, and gynecological disease treatments.[25–27] Moreover, it is the main herbal ingredient used in Jaseng wasahaepyo-tang, which is an herbal prescription for the treatment of facial nerve palsy. However, the anti-inflammatory action of LLT in cortical neurons has not been well examined. Based on the findings from several studies that highlighted the role of LLT in controlling inflammation, we therefore hypothesized that it might have a neurotherapeutic effect on H_2O_2-insulted cortical neurons by blocking NLRP3 inflammasome activation. This is the first report demonstrating the neurotherapeutic effect of LLT using an in vitro H_2O_2 model of cortical neurons, thus suggesting a new strategy for the utilization of this natural substance to treat various neurological diseases.

Materials and Methods

In vitro Culture of Cortical Neurons

All animals used in this study were maintained in accordance with the Jaseng Animal Care and Use Committee (JSR-2020-03-004). Primary cortical neurons were prepared according to previously published protocols from Sprague-Dawley rat embryos (embryonic day 17, Daehan Bio Link, Chungbuk, Korea).[28,29] Briefly, a pregnant female rat was sacrificed by CO_2-induced asphyxiation, and the embryos were promptly separated via cesarean section using large scissor and tooth forceps and placed in a 100 mm x 20 mm petri dish containing cold Hank's balanced salt solution (HBSS; Gibco BRL, Grand Island, NY, USA) on ice. Embryos were positioned with the dorsal side facing up and carefully fixed at the head/neck junction using fine forceps. The skin and skull on the head of the embryo were carefully removed with No. 5 fine forceps until the upper surface of the brain was visible. Moreover, the cerebral cortex was carefully isolated and placed in HBSS (Gibco), and the meninges were manually removed from the cerebral hemispheres (Supplementary Video S1). The tissues were rinsed twice in HBSS, digested with 2 mL of 2.5 mg/mL papain solution (Sigma-Aldrich, St. Louis, MO, USA) in HBSS for 15

min at 37°C, and the supernatant was discarded. The tissues were then rinsed twice in 2 mL HBSS and centrifuged at 1500 rpm for 3 min to obtain the cell pellet. Cells were triturated in 1 mL cortical neuron culture medium containing neurobasal medium (Gibco BRL) supplemented with 1% penicillin/streptomycin (Gibco BRL), 1% Gluta-MAX (Gibco BRL), and 2% B27 (right before using, Gibco BRL). Single cells were then seeded onto 12 mm circular cover slips for immunocytochemical analysis, a 6-well plate for fluorescence-activated cell sorting (FACS) analysis, and 96-well plates for the cell viability assay, which were then coated with 20 mg/mL poly-D-lysine (Gibco BRL) overnight, followed by 10 mg/mL laminin (Sigma-Aldrich) for 2 h at 4°C.

Preparation of LLT

The LLT extract was prepared according to a previously described method.[30] First, the original LLT (10 g) was heated to 105°C with water (300 mL) by refluxing for 3 h, cooled on ice, and filtered once with filter paper (Hyundai micro, HA-030, Korea). The filtrate was lyophilized using a freeze dryer (Ilshin BioBase, Korea) to obtain dry LLT extract; this extract was weighed, and the extract yield was calculated and re-dissolved in phosphate-buffered saline (PBS) to the high-dose concentration (10 mg/mL). The extract was moved to a conical flask and maintained at −70°C.

H_2O_2-Induced Neuronal Injury and LLT Treatment

Cortical neurons were plated at different densities on poly-D-lysine/laminin plates for various analyses (4×10^5 cells/450 µL in a 24-well-plate for immunocytochemistry (ICC); 2×10^6 cells/1.8 mL in a 6-well-plate for flow cytometry; 4×10^6 cells/2.7 mL in a 60 mm^2 dish for real-time PCR) for 2~3 h. After attachment and stabilization, H_2O_2 (Sigma-Aldrich, 5 mM) was added at 10% of the total volume to a final concentration of 500 µM. After 30 min, the H_2O_2-containing medium was discarded and replaced with new cortical culture medium containing various concentrations of LLT extract (10, 25, 50 µg/mL). The plates were then incubated in 5% CO_2 at 37°C for 24 h (Figure 1A shows the schematic diagram illustrating the experimental design). In addition, to assess the synaptic density and longest neurite length using a synaptic marker for ICC, the cells were prepared in 24-well plates at a density of 4×10^5 cells/450 µL and incubated for 7 days in vitro (DIV). The 7 DIV cortical neurons were treated and incubated for 24 h as described in Figure 1A.

Neuronal Viability Assay

Neuronal viability was analyzed using a Cell Counting Kit-8 (CCK-8; Dojindo, Kumamoto, Japan) at 24 h after treatment with LLT extract (1, 10, 25, 50, 100, 200, and 400 µg/mL) followed by stimulation with or without H_2O_2. Briefly, CCK-8 solution (10 µL) was added to each well and incubated for 4 h at 37°C, and then, absorbance was measured using a microplate reader (Epoch, BioteK, Winooski, VT, USA) at 450 nm. Neuronal viability was expressed as a percentage of the blank group which was defined as 100% viability. Neuronal viability was also determined using a live/dead cell imaging kit (Thermo Fisher Scientific, Waltham, MA, USA) according to the manufacturer's instructions. The staining solution comprised two probes measuring the recognized cytotoxicity and cell viability parameters calcein AM, indicating live cells (green), and BOBO-3 Iodide (EthD-1), indicating dead cells (red). The culture medium was discarded, and each sample was incubated in 100 µL of staining solution for 15 min at 37°C. To quantify neuronal viability, 10 random images per group were captured at 10× magnification using a confocal microscope (Eclipse C2 Plus, Minato, Tokyo, Nikon, Japan). Live and dead cells were manually counted using ImageJ software (1.37v, National Institutes of Health, Bethesda, MD, USA).

Immunocytochemistry

Changes in the expression of inflammatory factors related to the NLRP3 inflammasome in H_2O_2-treated cortical neurons were observed using ICC. The cells were assessed after 24 h of the LLT treatment with three different concentrations in H_2O_2-treated neurons. The samples were fixed with 4% paraformaldehyde for 30 min, rinsed three times with PBS for 5 min each, and then incubated with 0.2% triton X-100 in PBS for 5 min. After two rinses with PBS for 5 min and blocking with 2% normal goat serum in PBS for 1 h, the cells were incubated with primary antibodies diluted in 2% normal goat serum for overnight at 4°C. The primary antibodies used were as follows: NLRP3 (1:100; Abcam, Cambridge, MA, USA), ASC (1:200; Santa Cruz Biotechnology, CA, USA), Caspase-1 (1:200; Abcam), IL-1β (1:200; Novus Biologicals, CO, USA), brain-derived neurotrophic factor (BDNF; 1:200; Abcam), nerve growth factor (NGF; 1:100; Abcam), Synaptophysin (1:500; Sigma-Aldrich), and Tuj1 (1:2000; R&D systems,

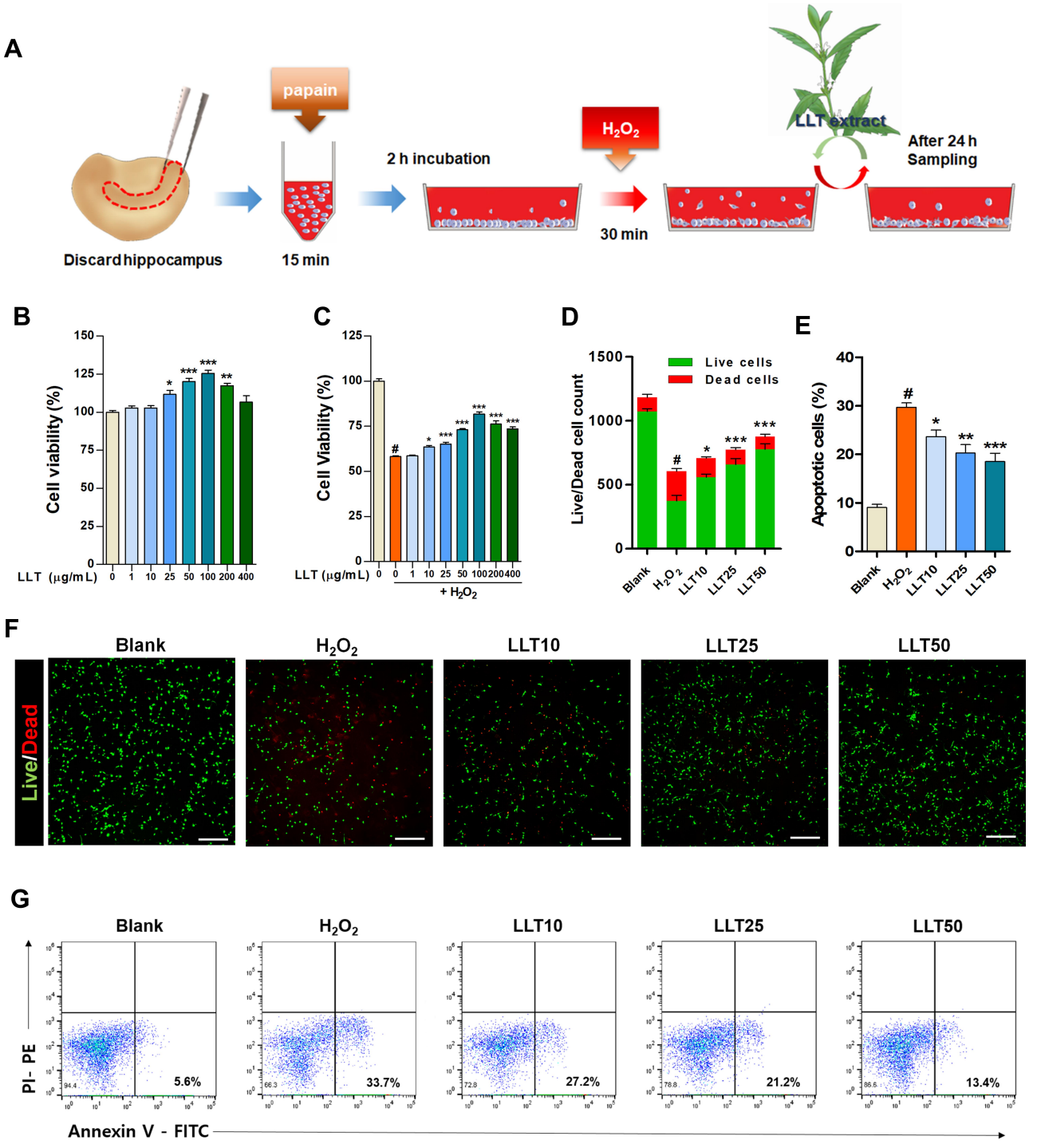

Figure 1 LLT protects cortical neurons against H_2O_2-induced neuronal damage. (**A**) Schematic depiction of experimental design for primary cortical neurons (**B**) Cell viability assay results of cortical neurons treated with various concentrations of LLT without H_2O_2 induction at 24 h, n = 3. (**C**) CCK-8 results of H_2O_2-treated cortical neurons treated with various concentrations of LLT at 24 h, n = 3. (**D**) The total number of live and dead cells calculated from cellular fluorescence images of each group. n = 10. (**E**) The percentage of apoptotic cells analyzed by flow cytometry of Annexin-V-FITC/PI-PE double staining. n = 5. (**F**) Fluorescence images of live and dead (red) cells for analysis of the neuroprotective effect of LLT at different concentrations on H_2O_2-treated cortical neurons. Scale bar = 200 μm. (**G**) Representative flow cytometric plot using Annexin-V/PI to confirm the mode of cell death. Blank = non-treatment, H_2O_2 = H_2O_2 only, LLT = H_2O_2+LLT extract. Significant differences are indicated as follows and were analyzed via one-way ANOVA with Tukey's post-hoc test: $^{\#}p < 0.001$ vs the blank group; $^{*}p < 0.05$, $^{**}p < 0.01$, and $^{***}p < 0.001$ vs the H_2O_2 group.

McKinley Place NE, USA). After three washes with PBS for 5 min each, the cells were incubated with fluorescent conjugated secondary antibodies (FITC-conjugated goat anti-rabbit IgG, FITC-conjugated goat anti-mouse IgG, Rhodamine Red-X-conjugated goat anti-rabbit IgG, Rhodamine Red-X-conjugated goat anti-mouse IgG,

Jackson Immuno-Research Labs, West Grove, PA, USA) diluted at 1:300 in 2% NGS for 2 h. After 2h of incubation at room temperature, the cells were washed three times for 5 min with PBS. The samples were treated with 4−6-diamidino-2-phenylindole (DAPI; Tokyo Chemical Industry Co., Tokyo, Japan) containing PBS for 10 min at room temperature. Next, the cells were washed three times with PBS for 5 min, mounted with fluorescence mounting medium (Dako Cytomation, Carpinteria, CA, USA), and imaged using a confocal microscope (Eclipse C2 Plus, Nikon). To quantify fluorescence intensity, 10 representative images were captured at 100× or 400× magnification using confocal microscopy with fixed acquisition settings. The average intensity was measured using Image J software (1.37 v, National Institutes of Health) and compared quantitatively. Synaptic density was quantified by the number of synaptophysin (Syn)-positive pixels, using ImageJ software. Then, the number of Syn-positive pixels was divided by the total number of pixels to calculate the mean percent Syn-labeled pixels.

Real-Time PCR

We analyzed the changes in the expression level of genes related to neuroinflammation and neuronal growth in each group using the real-time PCR technique. Total RNA was isolated from cells using Trizol reagent (Thermo Fisher Scientific), and cDNA was synthesized using random hexamer primers and Accupower RT premix (Bioneer, Korea). All primer pairs were designed using UCSC Genome Bioinformatics and the NCBI database (Table 1). Real-time PCR was performed using iQSYBR green Supermix (Bio-Rad, Hercules, CA, USA) on an CFX Connect Real-Time PCR Detection System (Bio-Rad), using the following conditions: an initial cycle of 3 min at 95°C, followed by 45 cycles of 15 s at 95°C and 30 s at 60°C. Each assay was performed at least three times. Target gene expression was normalized to *GAPDH* levels and expressed as a fold-change relative to the control.

Table 1 Primer Sequences Used for Real-Time PCR Analysis

Gene	5′-3′	Primer Sequence
Akt1	Forward Reverse	ACCTCTGAGACCGACACCAG AGGAGAACTGGGGAAAGTGC
BDNF	Forward Reverse	CTTGGAGAAGGAAACCGCCT GTCCACACAAAGCTCTCGGA
Caspase-1	Forward Reverse	ACTCGTACACGTCTTGCCCTCA CTGGGCAGGCAGCAAATTC
iNOS	Forward Reverse	ATGGCTTGCCCCTGGAAGTT TGTTGGGCTGGGAATAGCAC
IL-1β	Forward Reverse	TTGCTTCCAAGCCCTTGACT GGTCGTCATCATCCCACGAG
IL-18	Forward Reverse	GGACTGGCTGTGACCCTATC TGTCCTGGCACACGTTTCTG
NT3	Forward Reverse	CCGACAAGTCCTCAGCCATT CAGTGCTCGGACGTAGGTTT
NGF	Forward Reverse	CCAAGGACGCAGCTTTCTATC CTGTGTCAAGGGAATGCTGAAG
NLRP3	Forward Reverse	GCTCCAACCATTCTCTGACC AAGTAAGGCCGGAATTCACC
mTOR	Forward Reverse	GCAATGGGCACGAGTTTGTT AGTGTGTTCACCAGGCCAAA
GAPDH	Forward Reverse	CCCCCAATGTATCCGTTGTG TAGCCCAGGATGCCCTTTAGT

Flow Cytometry

The mode of cell death was determined using flow cytometry. Apoptotic cell death was detected using an Annexin V-Fluorescein isothiocyanate (FITC) propidium iodide (PI)-phycoerythrin[14] apoptosis detection kit (Abcam) as described previously. The cells were isolated with a cell scraper and centrifuged at 2000 rpm for 3 min. Briefly, cells were incubated with 1% Annexin V and 1% PI in binding buffer for 10 min and then analyzed directly using FACS (Accuri C6 plus flow cytometer, BD Biosciences, Franklin Lakes, NJ, USA) after adding the same volume of PBS.

Statistical Analysis

All results are expressed as the mean ± standard error of the mean. Comparisons among each group were analyzed using one-way analysis of variance (ANOVA) with Tukey's post-hoc test (Graph-Pad Prism, California, USA). Differences were considered statistically significant based on the following comparisons: # $p < 0.001$ vs the blank group and * $p < 0.05$, ** $p < 0.01$, or *** $p < 0.001$ vs the H_2O_2 group.

Results

LLT Protects Cortical Neurons Against H_2O_2-Induced Neuronal Death

First, we investigated the induction of neuronal death in cortical neurons upon H_2O_2 exposure, confirmed whether

LLT extract was non-toxic to cortical neurons, and evaluated the optimal therapeutic dose range of LLT by screening cell viability. A schematic illustration shows the experimental design of this study (Figure 1A). When setting the optimal H_2O_2 concentration and incubation period to induce neuronal damage, cell viability was checked by ICC for concentrations of 100 and 500 μM H_2O_2 with an incubation period of 30 min and 1 h (Supplementary Figure 1). The incubation of neurons with 100 μM H_2O_2 for 30 min induced mild neuronal injury. However, more severe neuronal injury was induced by exposure to 500 μM H_2O_2 for 30 min. Substantial neuronal injury was detected, with very low viability, at 1 h after initiating treatment with both 100 and 500 μM H_2O_2. We therefore chose the concentration and incubation period of 500 μM and 30 min, respectively, as suggested by a previous report,[31] to induce neuronal damage in cortical neurons. Cortical neurons were cultured with LLT (0, 10, 25, 50 μg/mL) 24 h after subjecting them to 500 μM H_2O_2 for 30 min to examine the effect of LLT on the suppression of neuroinflammation and NLRP3 inflammasome activation by immunological and molecular-biological analysis. LLT extract alone was not toxic to cortical neurons at concentrations ranging from 1 to 400 μg/mL and significantly increased cell viability compared to that in the control group at 25 to 200 μg/mL (Figure 1B). The optimal concentration for this neuroprotective effect was evaluated 24 h after H_2O_2-treated neurons had been treated with LLT. We found that neuronal viability decreased to approximately 60% when cortical neurons were treated with H_2O_2 (500 μM; Figure 1C); however, treatment with LLT (1 to 400 μg/mL) for 24 h significantly and dose-dependently increased neuronal viability. These findings demonstrate that LLT extract has neuroprotective effects on H_2O_2-induced neuronal injury.

Live/dead cell assays were also performed to quantify the live (green) and dead (red) cells under the same culture conditions. The neurons treated with LLT were mostly positive for calcein-AM (green fluorescence), indicating that LLT significantly and dose-dependently increased the number of live cells compared to that in the H_2O_2 group (Figure 1D and F). We further confirmed the mode of neuronal death using flow cytometry with the calcium-dependent phospholipid adhesion protein, Annexin V, to confirm apoptosis, and PI to detect late apoptosis/necrosis (Figure 1E and G). When treated with H_2O_2, more primary cultured cortical neurons underwent apoptosis (Annexin V +/PI−); however, LLT decreased the population of apoptotic cells induced by H_2O_2 in a dose-dependent manner. Therefore, we examined the inhibitory effects of LLT extract on H_2O_2-induced neuronal death in cortical neurons.

Effect of LLT on H_2O_2-Induced Neuroinflammation in Cortical Neurons

To assess the effect of LLT extract on iNOS expression, a major mediator of inflammation, we examined iNOS expression in H_2O_2-induced neurons using ICC (Figure 2A). iNOS expression was substantially increased by H_2O_2 treatment but significantly decreased by LLT (Figure 2B). Consistently, *iNOS* mRNA expression was also markedly higher in the H_2O_2 group and significantly decreased by LLT in a dose-dependent manner (Figure 2C). Then, we assessed whether LLT treatment regulates IL-6 and IL-10 cytokine release in the culture medium using cytokine-specific ELISAs. IL-6 is another proinflammatory cytokine known to be present in neurons and plays a key role in the neuronal injury response.[32] The level of IL-6 was upregulated in the H_2O_2 group, whereas a much lower level of IL-6 was detected in the LLT groups. In particular, IL-6 levels in the medium were subjected to a significant LLT-dose dependent effect (Figure 2D). Moreover, LLT enhanced the expression of the anti-inflammatory cytokine IL-10 and led to a dose-dependent induction in cortical neurons (Figure 2E). Based on these results, the application of LLT to cortical neurons inhibited the inflammatory response by decreasing the expression of proinflammatory cytokines (iNOS and IL-6) and increasing the expression of an anti-inflammatory cytokine (IL-10).

Effect of LLT on NLRP3 Inflammasome Activation in Cortical Neurons

To determine whether LLT extract inhibits NLRP3 inflammasome activation in neurons, we used ICC to assess the expression of NLRP3 inflammasomes (Figure 3A), which were identified morphologically as dots inside the cell body. H_2O_2 treatment strongly enhanced NLRP3 inflammasome expression in the neuronal cell body and increased the percentage of $NLRP3^+$ neurons by approximately 20% compared to that in the groups treated with LLT, which significantly and dose-dependently inhibited NLRP3 expression (Figure 3C). We also examined *NLRP3* mRNA expression using real-time PCR following H_2O_2 treatment and 24 h after LLT treatment in H_2O_2-treated cortical neurons (Figure 3D). *NLRP3* mRNA expression was significantly higher in the

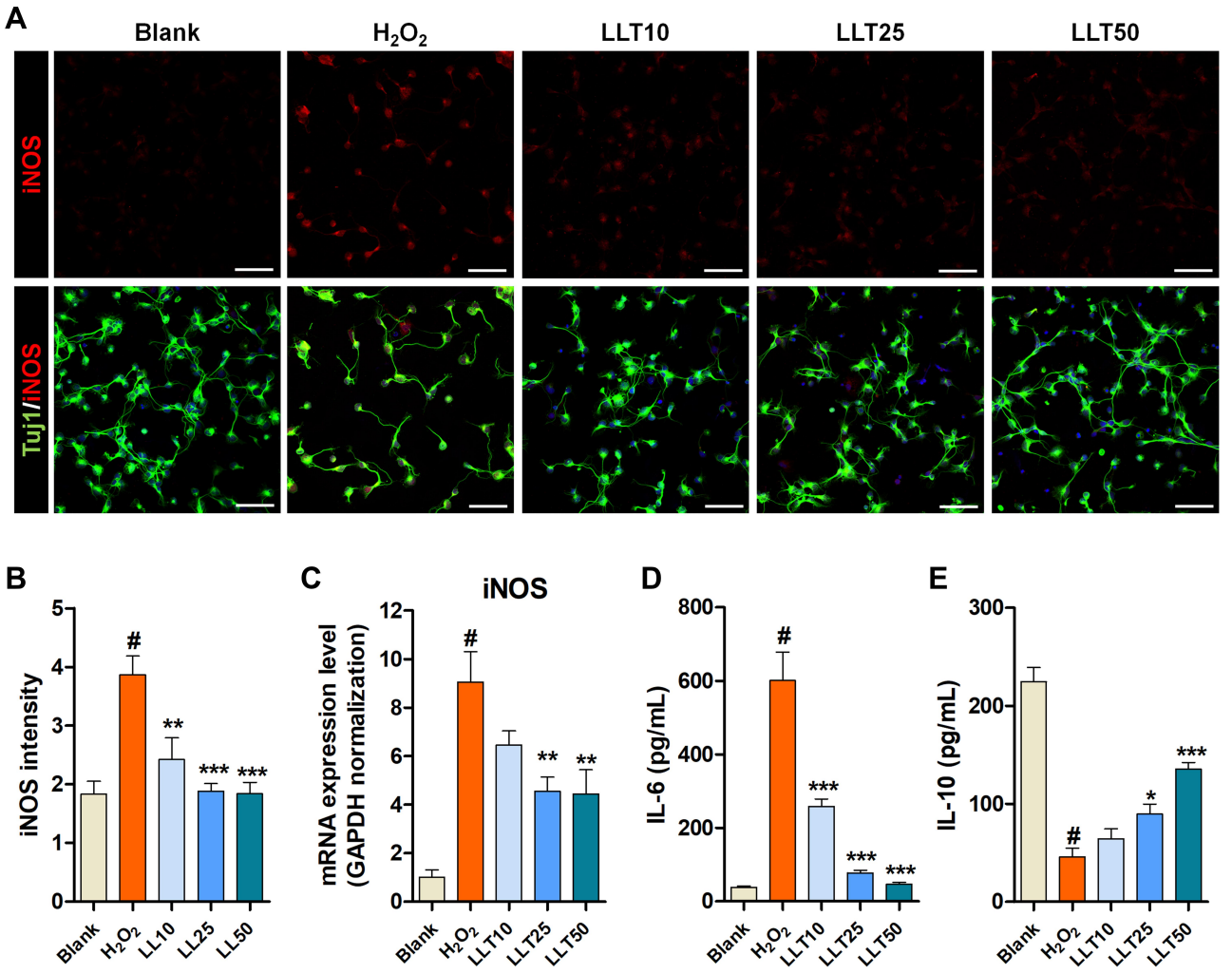

Figure 2 LLT suppresses inflammatory responses in H_2O_2-treated cortical neurons. (**A**) Representative images of iNOS (red) for analysis of inflammatory response in H_2O_2 -treated cortical neurons after LLT treatment, stained with Tuj1 for neurites and DAPI (blue) for nuclei. Scale bar = 50 μm. (**B**) The relative intensity of iNOS per field of view was quantified from iNOS fluorescence images of each group. n = 6. (**C**) Quantitative data from real-time PCR for iNOS after LLT treatment under H_2O_2 conditions. (**D**, **E**) The levels of IL-6 (**D**) and IL-10 (**E**) in the culture medium determined by ELISA, n = 6; Blank = non-treatment, H_2O_2 = H_2O_2 only, LLT = H_2O_2+LLT extract. Significant differences were analyzed via one-way ANOVA with Tukey's post-hoc test and are indicated as follows: $^{\#}p < 0.001$ vs the blank group; $^{*}p < 0.05$, $^{**}p < 0.01$, and $^{***}p < 0.001$ vs the H_2O_2 group.

H_2O_2 group than in the blank group; however, LLT dose-dependently decreased *NLRP3* mRNA expression in H_2O_2-treated cortical neurons.

Inflammasomes form protein domain bonds with caspase-1 either directly or via the adapter protein ASC; therefore, inflammatory activity causes a multi-step association with Nod-like receptors and the IL-1β cleavage enzyme caspase-1 through ASC.[33] Consequently, we analyzed ASC expression using ICC, observing a correlation with the ICC staining result for NLRP3 (Figure 3B). Moreover, the number of cells expressing ASC was significantly higher in the H_2O_2 group than in the blank group and was lower following LLT treatment (25 and 50 μg/mL; Figure 3E). Consistently, *ASC* mRNA expression was significantly higher in the H_2O_2 group than in the control group and decreased following LLT treatment in a dose-dependent manner (Figure 3F). In addition, we have performed double staining with a combination of NLRP3 and ASC antibodies to more directly confirm the inhibitory effect of LLT on the formation of the NLRP3-ASC complex (Supplementary Figure 2). NLRP3 expression and distribution as dot morphology in the nucleus were markedly increased in the H_2O_2 group compared to those in the blank group. Particularly for ASC expression, even strongly positive NLRP3 neurons were also strongly positive for ASC in the cytoplasm. Thus, both NLRP3 and ASC expression were strongly positive when neurons were treated with H_2O_2. Meanwhile, treatment with LLT

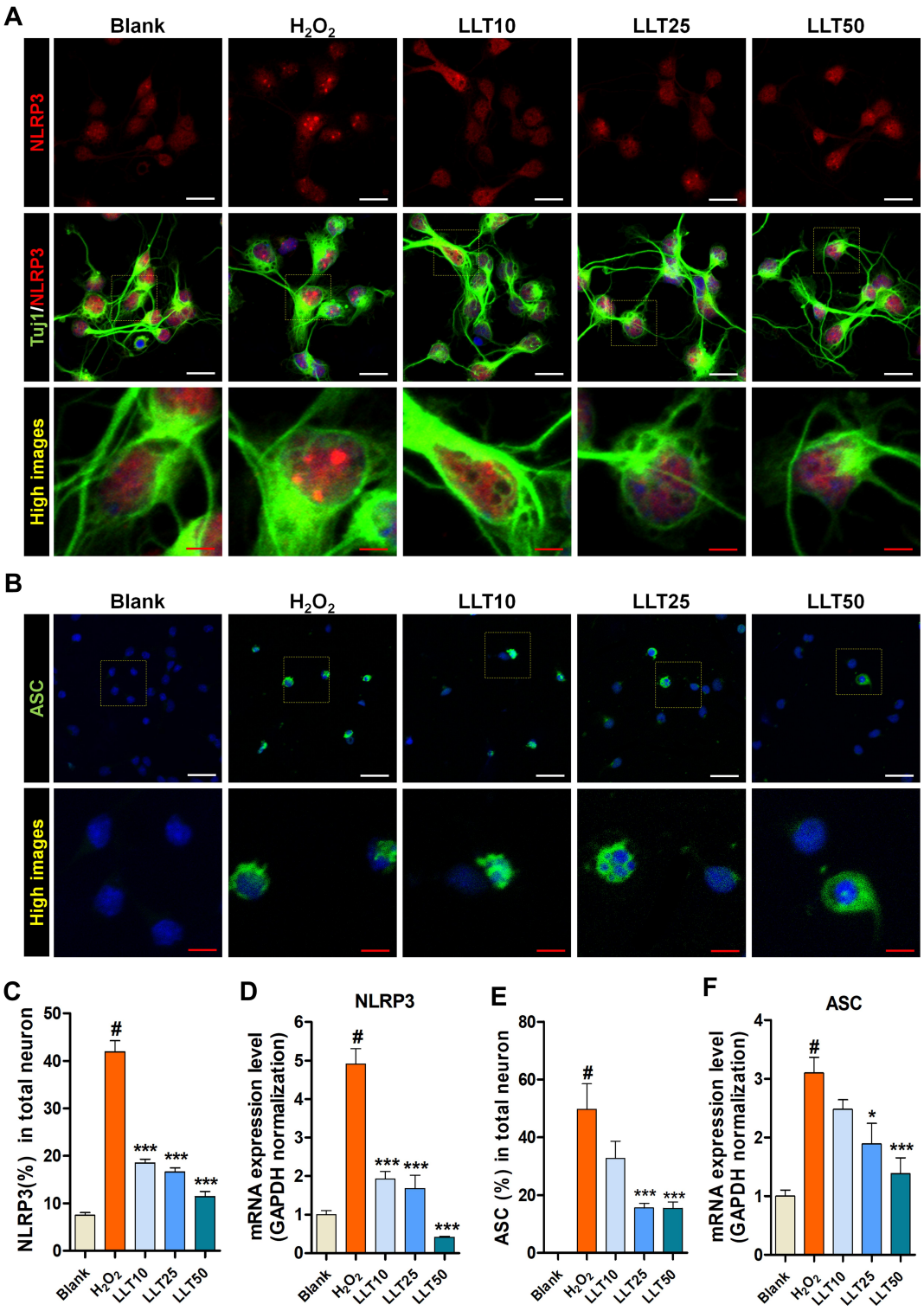

Figure 3 LLT inhibits NLRP3-ASC activation by H_2O_2 in cortical neurons. (**A**) Representative immunocytochemical images of NLRP3 inflammasome (red) in H_2O_2-treated cortical neurons after LLT treatment, stained with Tuj-1 for neurites and DAPI (blue) for nuclei. (**B**) ASC following H_2O_2 treatment and applying various concentrations of LLT, stained with DAPI (blue) for nuclei. White scale bar = 50 μm, red scale bar = 20 μm. (**C**) The relative percentage of NLRP3-positive neurons for the primary cortical neurons of blank, H_2O_2, and LLT groups (10, 25, 50 μg/mL) at 24 h. (**D**) Quantitative data from mRNA analysis of *NLRP3* levels in LLT groups compared with the H_2O_2 group. (**E**) The relative percentage of ASC-positive neurons for the primary cortical neurons of blank, H_2O_2, and LLT groups at 24 h. (**F**) Quantitative data from mRNA analysis of *ASC* levels in LLT groups compared with the H_2O_2 group, n = 6; blank = non-treatment, H_2O_2 = H_2O_2 only, LLT = H_2O_2+LLT extract. Significant differences were analyzed via one-way ANOVA with Tukey's post-hoc test and are indicated as follows: $^{\#}p < 0.001$ vs the blank group; $^{*}p < 0.05$, and $^{***}p < 0.001$ vs the H_2O_2 group.

decreased this expression, and trends showed a reduction. Next, we strive to clarify these causal relationships and moderating effects of LLT on NLRP3-ASC complex using immunoprecipitation (IP) assay. The IP results revealed that the same amount of ASC in neuron lysate of H_2O_2 group could bind more NLRP3 and pro-caspase-1 to initiate NLRP3 inflammasome than LLT groups (Supplementary Figure 3). Therefore, LLT extract appears to effectively inhibit ASC-dependent NLRP3 inflammasome activation in cortical neurons.

Effect of LLT on Caspase-1 and IL-1β Secretion via the NLRP3 Inflammasome Pathway

The inflammasome is a multiprotein complex that mediates caspase-1 activation, which subsequently promotes secretion of the proinflammatory cytokines IL-1β and IL-18.[34] Therefore, we examined caspase-1 activation in cortical neurons using fluorescence-based ICC with specific antibodies (Figure 4A). Caspase-1 fluorescence intensity was significantly increased by H_2O_2 treatment; however, this effect was inhibited by LLT treatment (Figure 4B). Subsequent analysis of *caspase-1* mRNA expression after LLT treatment in H_2O_2-treated cortical neurons confirmed that its expression was significantly higher in the H_2O_2 group than in the blank group and was downregulated significantly and dose-dependently by LLT treatment (Figure 4C).

We also examined IL-1β levels using ICC in the H_2O_2 and LLT-treated groups (Figure 4D), finding that the relative intensity of IL-1β was elevated after H_2O_2 treatment but reduced in a dose-dependent manner in the LLT group (Figure 4E). Real-time PCR analysis of *IL-1β* and *IL-18* gene expression confirmed that H_2O_2 treatment significantly increased the relative mRNA levels of both, whereas all LLT doses significantly downregulated their mRNA expression in a dose-dependent manner (Figure 4F and G). Therefore, these findings confirm that LLT can inhibit caspase-1 expression mediated by inflammasome action and block IL-1β and IL-18 secretion upon H_2O_2-induced neuronal damage.

Effect of LLT on Neurotrophic Factor Induction in H_2O_2-Treated Cortical Neurons

Neurotrophic factors stimulate neuroprotection and thus have been classically considered a good source of treatments for neurodegenerative diseases. BDNF and NGF are powerful factors associated with neuroprotection and neuroplasticity.[35] We found that neurons treated with H_2O_2 displayed significantly lower BDNF and NGF expression, whereas LLT treatment dose-dependently increased BDNF and NGF expression (Figure 5A and B). Similarly, image-based quantification revealed that LLT treatment significantly increased BDNF and NGF expression intensity (Figure 5C and D), and the mRNA level of *BDNF* was also significantly and dose-dependently increased after LLT treatment upon H_2O_2-induced neuronal damage (Figure 5E). *NGF* was also dramatically decreased in H_2O_2 groups. However, *NGF* gene expression was not changed after the application of 10 μg/mL LLT but significantly increased with 25 and 50 μg/mL LLT (Figure 5F).

Real-time PCR yielded results consistent with those of ICC experiments, confirming that LLT exerts protective effects against H_2O_2-induced neuronal damage, promoting nerve function restoration by increasing the expression of neurotrophic factors such as BDNF and NGF. In addition, we confirmed that LLT treatment alone, without H_2O_2, significantly increased $BDNF^+$ (Supplementary Figure 4A and B) and NGF^+ (Supplementary Figure 4C and D) cortical neurons, as indicated by FACS. Together, these results suggest that the therapeutic effects of increased BDNF and NGF secretion could effectively stimulate the regrowth of injured axons.

Neuroprotective Effect of LLT on Synapse Formation in H_2O_2-Treated Cortical Neurons

Synaptogenesis describes the critical process of synapse formation between neurons that allows for the assembly of neuronal circuits. Syn is a major synaptic protein used as a biomarker of synaptogenesis in cultured neurons.[36] We confirmed Syn expression in H_2O_2-treated cortical neurons after LLT treatment and found that its expression was promoted by LLT but abolished by H_2O_2 (Figure 6A). The synaptic densities per field of view was greater in the LLT groups than in the H_2O_2 group (Figure 6B). In addition, we compared the longest neurite lengths in cortical neurons after treatment with various concentrations of LLT under H_2O_2 conditions by determining Tuj1 immunoreactivity at 7 DIV (Figure 6C). Notably, LLT enhanced axonal elongation compared to that with H_2O_2 and significantly and dose-

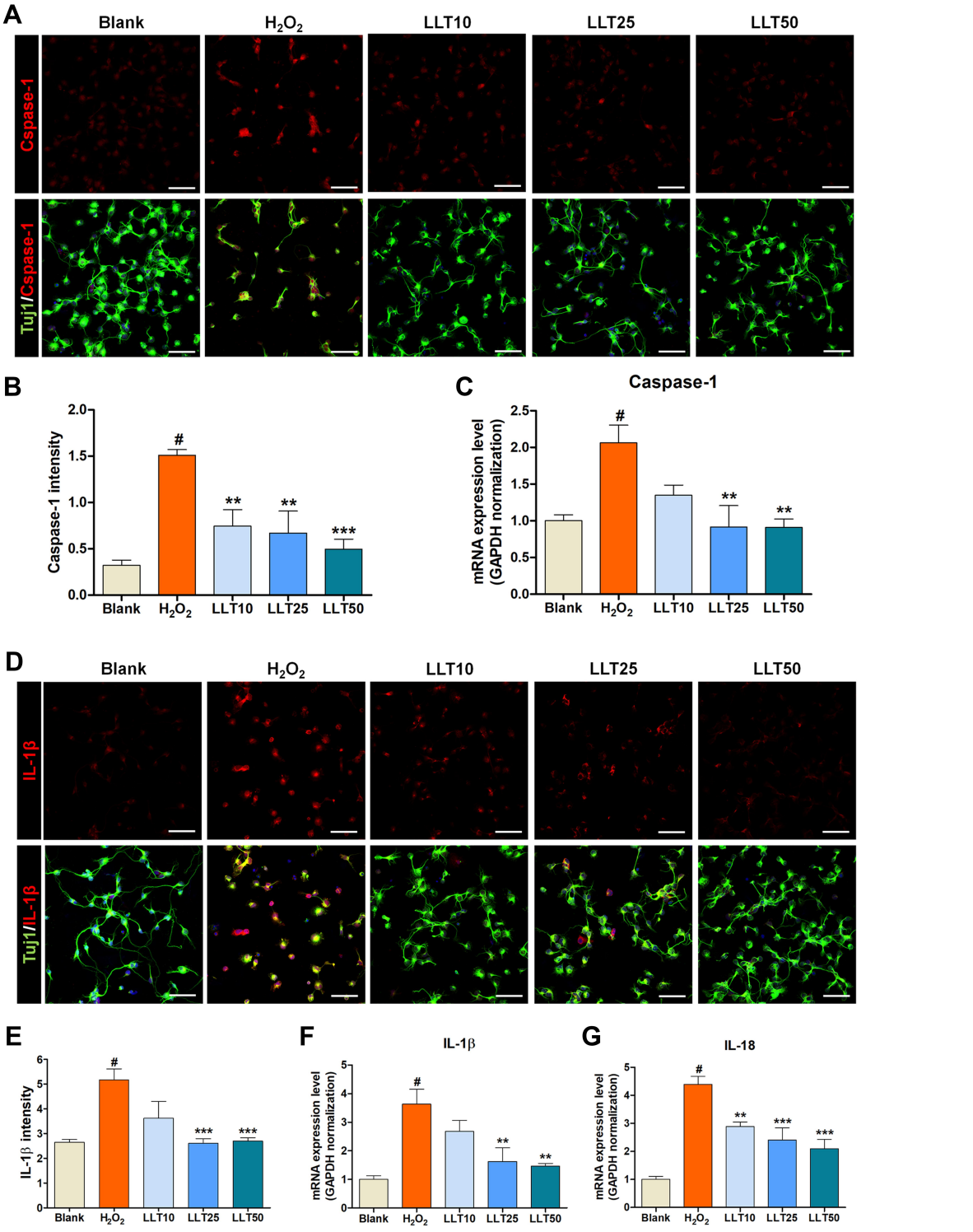

Figure 4 LLT inhibits IL-1β and caspase-1 activation triggered by the NLRP3 inflammasome. (**A**) Representative fluorescence images of primary cortical neurons stained with caspase-1 (red), Tuj-1 for neurites, and DAPI (blue) for nuclei in each group. Scale bar = 50 μm. (**B**) The quantitative representation of changes in caspase-1 intensity after LLT treatment at various concentrations. n = 6. (**C**) Quantitative data from real-time PCR for *caspase-1* in each group, n = 6. (**D**) Representative fluorescence images of IL-1β (red) in H_2O_2-treated cortical neurons after LLT treatment, stained with Tuj-1 for neurites and DAPI (blue) for nuclei. Scale bar = 50 μm. (**E**) The quantitative representation of changes in IL-1β intensity after LLT treatment at various concentrations. n = 6. (**F** and **G**) Quantitative data from real-time PCR for *IL-1β* (**F**) and *IL-18* (**G**) in each group n = 6; blank = non-treatment, H_2O_2 = H_2O_2 only, LLT = H_2O_2+LLT extract. Significant differences were analyzed via one-way ANOVA with Tukey's post-hoc test and are indicated as follows: $^{\#}p < 0.001$ vs the blank group; $^{**}p < 0.01$, and $^{***}p < 0.001$ vs the H_2O_2 group.

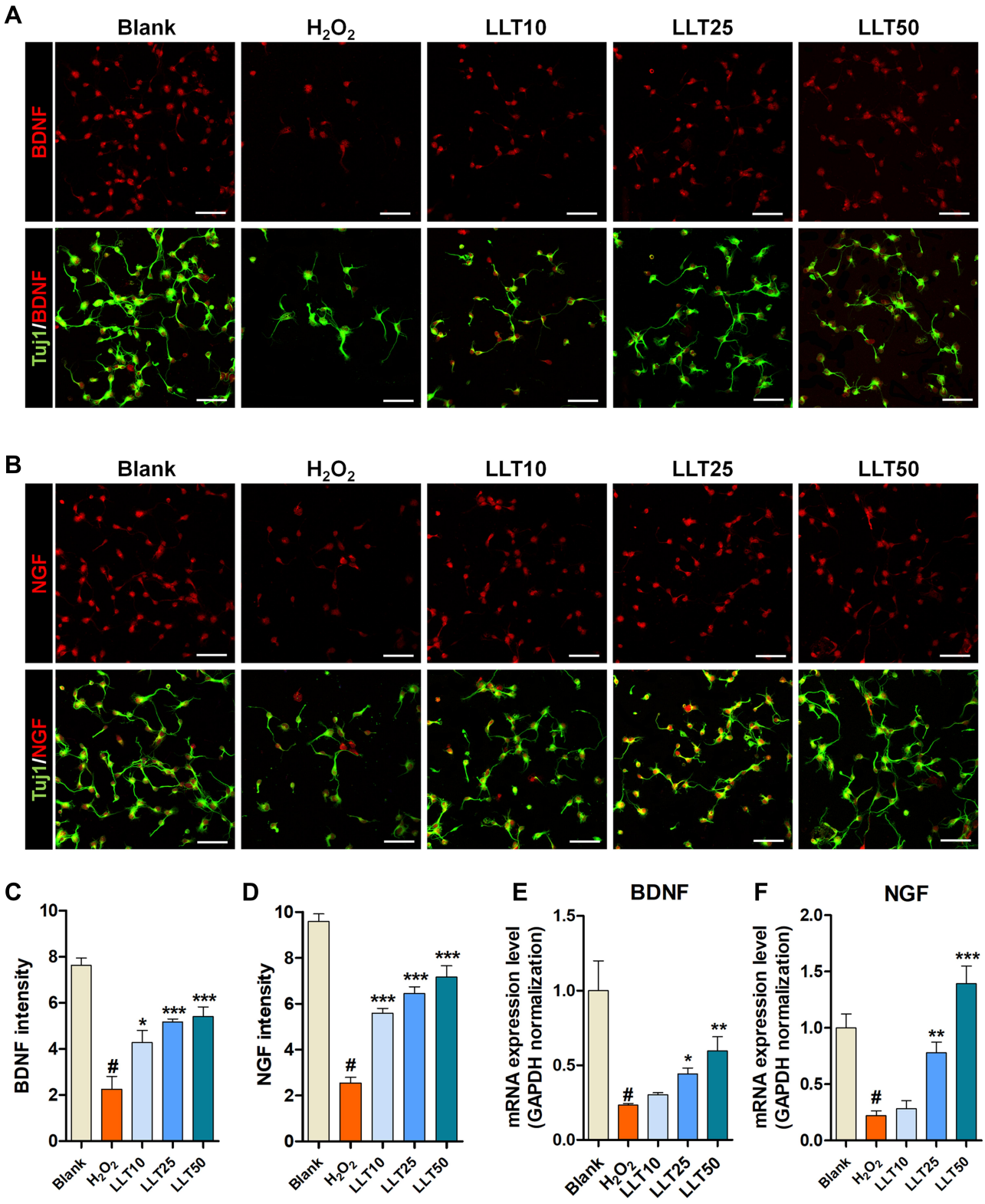

Figure 5 LLT enhances neurotrophic factor expression in H_2O_2-treated cortical neurons. (**A**) Representative fluorescence images of primary cortical neurons stained with BDNF (red) and Tuj-1 in each group. (**B**) Representative fluorescence images of primary cortical neurons stained with NGF (red) and Tuj-1 in each group. (**C** and **D**) Quantification of (**C**) BDNF and (**D**) NGF intensities based on immunofluorescence images using ImageJ. n = 6. (**E** and **F**) Relative quantification of (**E**) *BDNF* and (**F**) *NGF* genes by real-time PCR in each group. n = 6; blank = non-treatment, H_2O_2 = H_2O_2 only, LLT = H_2O_2+LLT extract. Significant differences were analyzed via one-way ANOVA with Tukey's post-hoc test and are indicated as follows: $^{\#}p < 0.001$ vs the blank group; $^{*}p < 0.05$, $^{**}p < 0.01$, and $^{***}p < 0.001$ vs the H_2O_2 group.

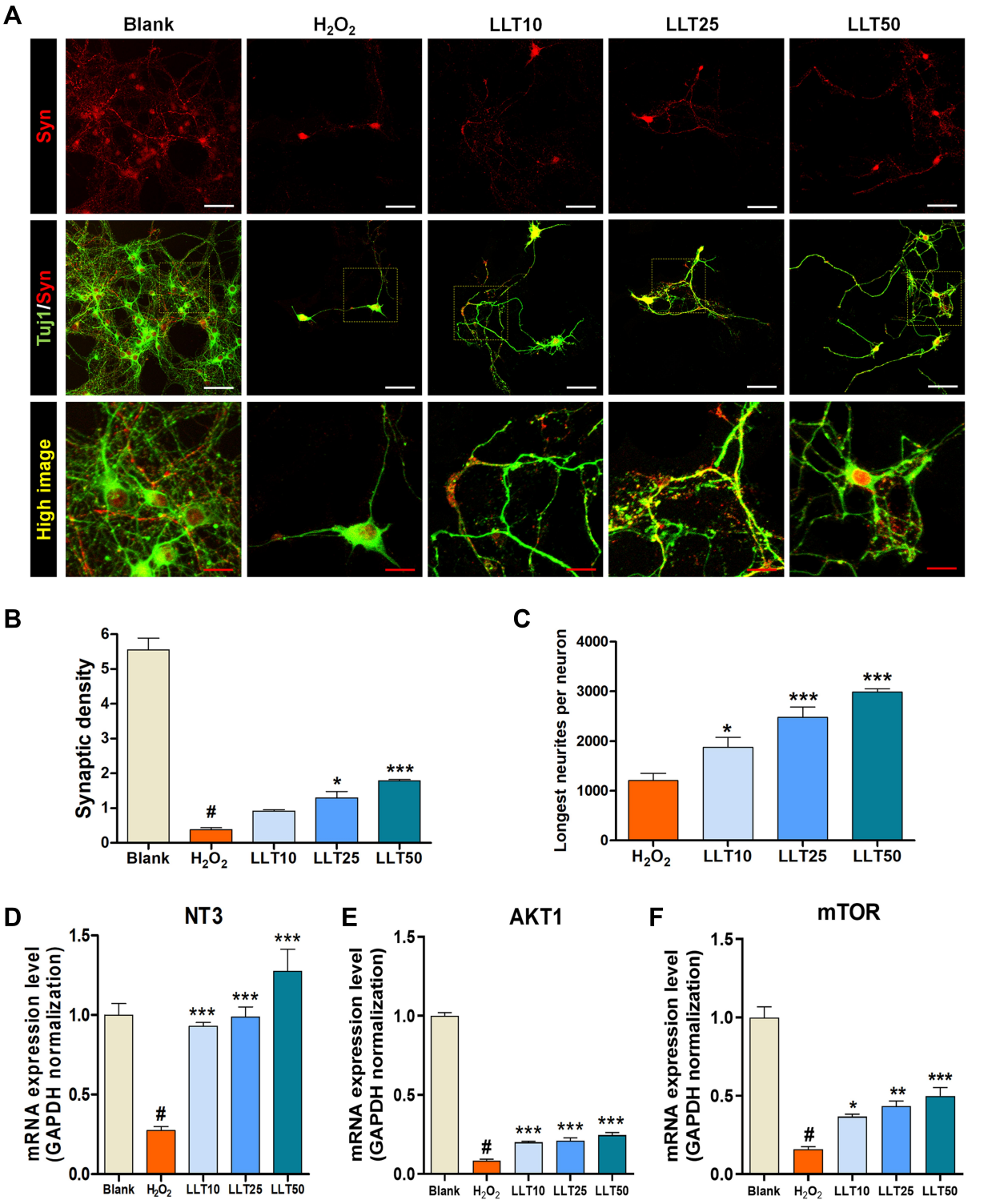

Figure 6 LLT enhances the axonal regrowth and synaptic connection in H_2O_2-treated cortical neurons. (**A**) Representative fluorescent images of synaptophysin (red) expression in Tuj1-positive neurons treated with LLT under H_2O_2 conditions at 7 days. White scale bar = 50 μm, red scale bar = 20 μm. (**B**) Quantitative analysis of synaptic density per field of view in cortical neurons treated with LLT in the presence of H_2O_2. (**C**) Quantitative analysis of the longest neurite length per field of view in cortical neurons treated with LLT under H_2O_2 conditions, n = 6. (**D**–**F**) Relative quantification from real-time PCR data for neuronal growth-related genes, (**D**) *NT3*, (**E**) *AKT1*, and (**F**) *mTOR* at 24 h in H_2O_2-treated cortical neurons treated with LLT at various concentrations (5, 10, 20 μg/mL), n = 6; blank = non-treatment, H_2O_2 = H_2O_2 only, LLT = H_2O_2+LLT extract. Significant differences were analyzed via one-way ANOVA with Tukey's post-hoc test and are indicated as follows: $^{\#}p < 0.001$ vs the blank group; $^{*}p < 0.05$, $^{**}p < 0.01$, and $^{***}p < 0.001$ vs the H_2O_2 group.

dependently increased the length of the longest neurite. We also confirmed that LLT treatment, without H_2O_2, significantly increased the expression of synaptophysin in cortical neurons, as determined using FACS (Supplementary Figure 5). Neurotrophin 3 (NT3) is a neurotrophic factor belonging to the NGF family and has displayed neuroprotective effects.[37] We found that *NT3* mRNA expression was significantly higher in the LLT groups than in the H_2O_2 group and increased dramatically as the LLT dose increased (Figure 6D). The AKT1/mTOR signaling pathway is a well-known biomarker of neuroprotection and regeneration, and previous studies have reported that neuronal injury can be prevented due to neuroprotection by regulating AKT1/mTOR expression. We also performed mRNA expression analysis of the *AKT1* and *mTOR* genes (Figure 6E and F). These findings revealed that LLT treatment after H_2O_2 induction improved both dose-dependently, whereas *AKT1* and *mTOR* expression were decreased in the H_2O_2 group. Based on these results, increasing doses of LLT significantly enhanced axonal regrowth and synaptic connectivity with H_2O_2-induced neuronal injury in rat primary cortical neurons. Here, we summarize the neurotherapeutic effect of LLT through suppression of the NLRP3 inflammasome and apoptosis and by enhancing neurite outgrowth and synaptogenesis, as illustrated in Figure 7.

Discussion

LLT was one of the most effective herbal extracts and has been used as a traditional medicine for the treatment of general gynecological issues. These medicinal effects of LLT have been applied to treat various diseases and have been widely studied for their antioxidant and anti-inflammatory, anti-angiogenic, and wound healing effects, but the underlying mechanism remained poorly known. Here, we demonstrated that H_2O_2 treatment significantly induces NLRP3 inflammasome activation and eventually leads to proinflammatory cytokine responses in primary cortical neurons. Thus, the NLRP3 inflammasome pathway might be considered the key driver in H_2O_2-induced neuronal damage. Meanwhile, LLT efficiently inhibits H_2O_2-induced NLRP3 inflammasome activation in cortical neurons. In addition, LLT significantly reduced neuronal death through the inhibition of apoptosis and the secretion of proinflammatory cytokines in H_2O_2-treated cortical neurons, suggesting that it can be considered for therapeutic application against NLRP3-driven neurological diseases. NLRP3 inflammasome activation represents a common pathway for

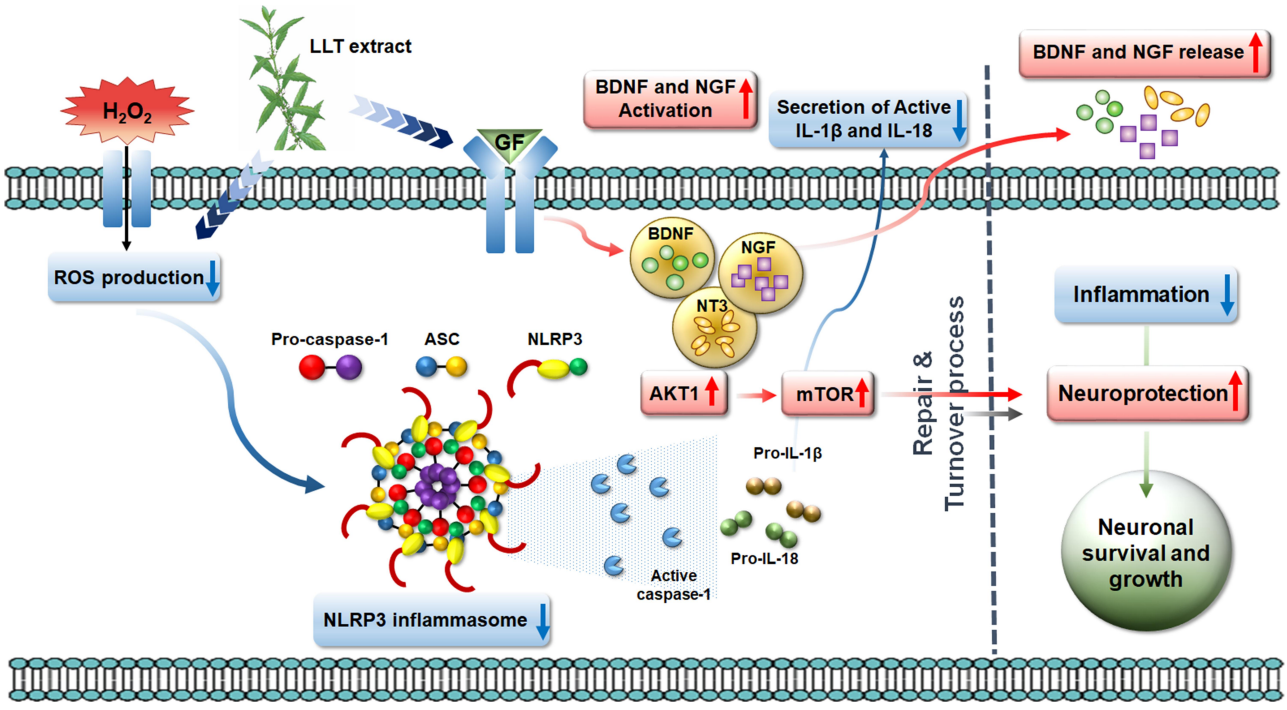

Figure 7 Schematic illustration showing the series of events associated with NLRP3 inflammasome activation in anti-inflammatory and neuroprotective effects of the LLT extract through ROS scavenging, the suppression of inflammation and apoptosis, enhancement of neuronal cell growth and axonal regeneration, and promotion of growth factor secretion.

a variety of diseases, including neurological, cardiovascular, psychiatric, metabolic, and inflammatory disorders.[38,39] Even though each disease displays distinct disease progression features, their progression has been related to the overactivation of inflammasome signaling, which contributes to neuroinflammation, metabolic alterations, and immune/inflammatory responses in such disorders. However, the preclinical in vivo studies are lacking in allowing for a better understanding of the pathophysiological role of NLRP3 in various pathological conditions. In support of the present study, in vivo NLRP3 modulation with LLT, acting on the NLRP3 inflammasome cascade in various neurological animal models, must be conducted to counteract the progression of central neuroinflammation, metabolic alterations, and immune/inflammatory responses. Based on these considerations, LLT is a stable natural product with a strong anti-inflammatory effect that does not exhibit cytotoxicity even at high concentrations, and it can be used very effectively for diseases related to neurological diseases in particular. Furthermore, by identifying the substance that induces axonal regeneration among the constituents of LLT, this will play an important role in the study of neural regeneration through the mechanism of NLRP3 inhibition.

Conclusion

Our findings demonstrate that LLT can effectively suppress the inflammatory response by inhibiting NLRP3 inflammasome activation and the secretion of caspase-1 and proinflammatory cytokines (IL-1β and IL-18), effectively alleviating or suppressing the mRNA expression of related factors. Therefore, LLT can promote neuronal survival and growth by exerting these neuroprotective effects on H_2O_2-induced neuronal injury.

Abbreviations

ANOVA, analysis of variance; CNS, central nervous system; FACS, fluorescence-activated cell sorting; HBSS, Hank's balanced salt solution; LLT, *Lycopus lucidus* Turcz; H_2O_2, hydrogen peroxide; PBS, phosphate buffered saline; PI, propidium iodide.

Ethics Approval

All animals used in this study were maintained in accordance with the Jaseng Animal Care and Use Committee (JSR-2020-03-004).

Funding

This research was funded by the Jaseng Medical Foundation, Korea.

Disclosure

The authors report no conflicts of interest in this work.

References

1. Kyritsis N, Kizil C, Brand M. Neuroinflammation and central nervous system regeneration in vertebrates. *Trends Cell Biol*. 2014;24(2):128–135. doi:10.1016/j.tcb.2013.08.004
2. Erickson MA, Dohi K, Banks WA. Neuroinflammation: a common pathway in CNS diseases as mediated at the blood-brain barrier. *Neuroimmunomodulation*. 2012;19(2):121–130. doi:10.1159/000330247
3. Chen L, Deng H, Cui H, et al. Inflammatory responses and inflammation-associated diseases in organs. *Oncotarget*. 2018;9(6):7204–7218. doi:10.18632/oncotarget.23208
4. Medzhitov R. Inflammation 2010: new adventures of an old flame. *Cell*. 2010;140(6):771–776. doi:10.1016/j.cell.2010.03.006
5. Saresella M, La Rosa F, Piancone F, et al. The NLRP3 and NLRP1 inflammasomes are activated in Alzheimer's disease. *Mol Neurodegener*. 2016;11(1):23. doi:10.1186/s13024-016-0088-1
6. Mantovani A, Dinarello CA, Molgora M, Garlanda C. Interleukin-1 and Related Cytokines in the Regulation of Inflammation and Immunity. *Immunity*. 2019;50(4):778–795. doi:10.1016/j.immuni.2019.03.012
7. Kelley N, Jeltema D, Duan Y, He Y. The NLRP3 Inflammasome: an Overview of Mechanisms of Activation and Regulation. *Int J Mol Sci*. 2019;20(13):3328. doi:10.3390/ijms20133328
8. Broz P, Dixit VM. Inflammasomes: mechanism of assembly, regulation and signalling. *Nat Rev Immunol*. 2016;16(7):407–420. doi:10.1038/nri.2016.58
9. Davis BK, Wen H, Ting JP. The inflammasome NLRs in immunity, inflammation, and associated diseases. *Annu Rev Immunol*. 2011;29:707–735. doi:10.1146/annurev-immunol-031210-101405
10. Yang Y, Wang H, Kouadir M, Song H, Shi F. Recent advances in the mechanisms of NLRP3 inflammasome activation and its inhibitors. *Cell Death Dis*. 2019;10(2):128. doi:10.1038/s41419-019-1413-8
11. Haque ME, Akther M, Jakaria M, Kim IS, Azam S, Choi DK. Targeting the microglial NLRP3 inflammasome and its role in Parkinson's disease. *Mov Disord*. 2020;35(1):20–33. doi:10.1002/mds.27874
12. Hong P, Gu RN, Li FX, et al. NLRP3 inflammasome as a potential treatment in ischemic stroke concomitant with diabetes. *J Neuroinflammation*. 2019;16(1):121. doi:10.1186/s12974-019-1498-0
13. Lee E, Hwang I, Park S, et al. MPTP-driven NLRP3 inflammasome activation in microglia plays a central role in dopaminergic neurodegeneration. *Cell Death Differ*. 2019;26(2):213–228. doi:10.1038/s41418-018-0124-5
14. Li SJ, Zhang YF, Ma SH, et al. The role of NLRP3 inflammasome in stroke and central poststroke pain. *Medicine*. 2018;97(33):e11861. doi:10.1097/MD.0000000000011861
15. Tan MS, Yu JT, Jiang T, Zhu XC, Tan L. The NLRP3 inflammasome in Alzheimer's disease. *Mol Neurobiol*. 2013;48(3):875–882. doi:10.1007/s12035-013-8475-x
16. Kuwar R, Rolfe A, Di L, et al. A novel small molecular NLRP3 inflammasome inhibitor alleviates neuroinflammatory response following traumatic brain injury. *J Neuroinflammation*. 2019;16(1):81. doi:10.1186/s12974-019-1471-y

17. Ismael S, Zhao L, Nasoohi S, Ishrat T. Inhibition of the NLRP3-inflammasome as a potential approach for neuroprotection after stroke. *Sci Rep*. 2018;8(1):5971. doi:10.1038/s41598-018-24350-x
18. Ismael S, Ahmed HA, Adris T, Parveen K, Thakor P, Ishrat T. The NLRP3 inflammasome: a potential therapeutic target for traumatic brain injury. *Neural Regen Res*. 2021;16(1):49–57. doi:10.4103/1673-5374.286951
19. Tungmunnithum D, Thongboonyou A, Pholboon A, Yangsabai A. Flavonoids and Other Phenolic Compounds from Medicinal Plants for Pharmaceutical and Medical Aspects: an Overview. *Medicines*. 2018;5(3).
20. Pandey KB, Rizvi SI. Plant polyphenols as dietary antioxidants in human health and disease. *Oxid Med Cell Longev*. 2009;2(5):270–278. doi:10.4161/oxim.2.5.9498
21. Cao Y, Zhang L, Sun S, Yi Z, Jiang X, Jia D. Neuroprotective effects of syringic acid against OGD/R-induced injury in cultured hippocampal neuronal cells. *Int J Mol Med*. 2016;38(2):567–573. doi:10.3892/ijmm.2016.2623
22. Ogut E, Sekerci R, Akcay G, et al. Protective effects of syringic acid on neurobehavioral deficits and hippocampal tissue damages induced by sub-chronic deltamethrin exposure. *Neurotoxicol Teratol*. 2019;76:106839. doi:10.1016/j.ntt.2019.106839
23. Rashedinia M, Alimohammadi M, Shalfroushan N, et al. Neuroprotective Effect of Syringic Acid by Modulation of Oxidative Stress and Mitochondrial Mass in Diabetic Rats. *Biomed Res Int*. 2020;2020:8297984. doi:10.1155/2020/8297984
24. Khojasteh A, Mirjalili MH, Alcalde MA, Cusido RM, Eibl R, Palazon J. Powerful Plant Antioxidants: a New Biosustainable Approach to the Production of Rosmarinic Acid. *Antioxidants*. 2020;9(12). doi:10.3390/antiox9121273
25. Jeong DW, Kim EY, Kim JH, et al. Lycopus lucidus Turcz Inhibits the Osteoclastogenesis in RAW 264.7 Cells and Bone Loss in Ovariectomized Rat Model. *Evid Based Complement Alternat Med*. 2019;2019:3231784. doi:10.1155/2019/3231784
26. Lee YJ, Kang DG, Kim JS, Lee HS. Lycopus lucidus inhibits high glucose-induced vascular inflammation in human umbilical vein endothelial cells. *Vascul Pharmacol*. 2008;48(1):38–46. doi:10.1016/j.vph.2007.11.004
27. Yu JQ, Lei JC, Zhang XQ, et al. Anticancer, antioxidant and antimicrobial activities of the essential oil of Lycopus lucidus Turcz. var. hirtus Regel. *Food Chem*. 2011;126(4):1593–1598. doi:10.1016/j.foodchem.2010.12.027
28. Pacifici M, Peruzzi F, Isolation and culture of rat embryonic neural cells: a quick protocol. *J Vis Exp*. 2012;63:e3965. doi:10.3791/3965
29. Shi H, Liu KJ. Effects of glucose concentration on redox status in rat primary cortical neurons under hypoxia. *Neurosci Lett*. 2006;410(1):57–61. doi:10.1016/j.neulet.2006.09.066
30. Kim SJ, Park B, Huh HW, et al. Achyranthis radix Extract-Loaded Eye Drop Formulation Development and Novel Evaluation Method for Dry Eye Treatment. *Pharmaceutics*. 2020;12(2):165. doi:10.3390/pharmaceutics12020165
31. Kim JW, Mahapatra C, Hong JY, et al. Functional Recovery of Contused Spinal Cord in Rat with the Injection of Optimal-Dosed Cerium Oxide Nanoparticles. *Adv Sci*. 2017;4(10):1700034. doi:10.1002/advs.201700034
32. Erta M, Quintana A, Hidalgo J. Interleukin-6, a major cytokine in the central nervous system. *Int J Biol Sci*. 2012;8(9):1254–1266. doi:10.7150/ijbs.4679
33. He Y, Hara H, Nunez G. Mechanism and Regulation of NLRP3 Inflammasome Activation. *Trends Biochem Sci*. 2016;41(12):1012–1021. doi:10.1016/j.tibs.2016.09.002
34. Franchi L, Eigenbrod T, Munoz-Planillo R, Nunez G. The inflammasome: a caspase-1-activation platform that regulates immune responses and disease pathogenesis. *Nat Immunol*. 2009;10(3):241–247. doi:10.1038/ni.1703
35. Weissmiller AM, Wu C. Current advances in using neurotrophic factors to treat neurodegenerative disorders. *Transl Neurodegener*. 2012;1(1):14. doi:10.1186/2047-9158-1-14
36. McAllister AK. Dynamic aspects of CNS synapse formation. *Annu Rev Neurosci*. 2007;30(1):425–450. doi:10.1146/annurev.neuro.29.051605.112830
37. Keefe KM, Sheikh IS, Smith GM. Targeting Neurotrophins to Specific Populations of Neurons: NGF, BDNF, and NT-3 and Their Relevance for Treatment of Spinal Cord Injury. *Int J Mol Sci*. 2017;18(3):548. doi:10.3390/ijms18030548
38. Fusco R, Siracusa R, Genovese T, Cuzzocrea S, Di Paola R. Focus on the Role of NLRP3 Inflammasome in Diseases. *Int J Mol Sci*. 2020;21(12):4223. doi:10.3390/ijms21124223
39. Pellegrini C, Fornai M, Antonioli L, Blandizzi C, Calderone V. Phytochemicals as Novel Therapeutic Strategies for NLRP3 Inflammasome-Related Neurological, Metabolic, and Inflammatory Diseases. *Int J Mol Sci*. 2019;20(12):2876. doi:10.3390/ijms20122876